Proc Indian Natn Sci Acad **80** No. 3 September 2014 pp. 513-524

DOI: 10.16943/ptinsa/2014/v80i3/55126

Review Article

A Review on Double-Diffusive Instability in Viscosity Stratified Flows

KIRTI CHANDRA SAHU*
Department of Chemical Engineering, Indian Institute of Technology Hyderabad, Yeddumailaram 502 205, Telangana, India

(Received on 7 March 2014; Revised on 31 May 2014; Accepted on 3 June 2014)

This is a review of the previous work conducted on the double-diffusive effect in viscosity stratified systems. Two configurations are considered which are supposed to be stable in the context of single-component flows. The flow in these configurations is shown to be unstable in the presence of double-diffusive effect. A new mode of instability due to the double-diffusive effect was found, and a rich variety of instability patterns are observed in the direct numerical simulations of such flows.

Key Word: Miscible Flow; Double-Diffusive Instability; Multiphase Flow; Mixing; Laminar Flow; Numerical Simulation; Linear Stability Analysis

Introduction

Double diffusive (DD) convection is a phenomenon frequently observed in the oceans and in many industrial situations (Govindarajan and Sahu, 2014). The "double-diffusive flow" means the flow in the presence of two species, which are diffusing at different rates. In this review, the instabilities that arise due to the double-diffusive effects in conditions which are supposed to be stable, according to our intuition, are discussed. The review is restricted to *viscosity-stratified* flows in two configurations, namely, core-annular/three-layer, and displacement flows. It is to be noted that the DD phenomena in *density-stratified* systems have been very well studied in the literature (see for example Turner, 1974), and this is not the subject of this review. However, a brief overview of double-diffusive phenomena in density stratified systems is given below, which will help us in understanding the underlying physics in the present systems.

Let us first imagine two situations: (i) a solid cone placed with its base on the ground, (ii) then the cone is inverted and placed with its nose on the ground. It is immediately obvious that the first situation is stable, while the second one is unstable. Similarly, a lighter fluid layer overlying a heavier fluid layer is stable, whereas if we invert it, the system becomes unstable. This is indeed true, except when there are multiple species (diffusing at different rates) in the system. Now let us imagine the ocean, where a layer of salty and warmer water lying above a layer of fresh and cold water, or the opposite. Since heat diffuses much faster than salt in water, the difference in diffusivity creates instabilities in the flow, which is discussed below.

Consider a warm salty layer of water which lies above a cold, fresh layer, and with a net density less than that of the bottom layer. This situation at first glance is 'stable'. However, since heat diffuses away faster, we will soon have a salty layer lying above a fresh water layer, at nearly the same temperature. This now is top-heavy and unstable, and fingers of salty water will start descending into the fresh layer. The length of these fingers increases at the rate at which heat diffuses away. This is the fingering mode of DD

*Author for Correspondence: ksahu@iith.ac.in; Tel: +91 40 2301 6053

instability. Now, let's consider the reverse, e.g. when a river has disgorged cold fresh water into the ocean. Suppose the original ocean water, which now lies below the cold fresh water from the river, is salty, warmer and denser than the river water. If a blob of river water is displaced downwards into the ocean water, being lighter than its surroundings, it will feel a buoyancy force pushing it back up, namely a stabilising effect. However, heat will diffuse away fast, and by the time the river water comes back to its original place, it will be warmer than it was before, and so lighter than its surroundings. It will therefore overshoot its original position, and this happening repeatedly means an oscillatory motion of increasing amplitude. This is termed the oscillatory mode of DD instability.

Recently, Govindarajan and Sahu (2014) reviewed the research work conducted on the instability in viscosity stratified flows of miscible and immissible fluids. In the present review, we will only discuss the instabilities due to the double-diffusive effect in viscosity stratified flows of two miscible fluids. The density is assumed to be the same everywhere in the flow. Two configurations are considered: (i) core-annular/three-layer flow, shown in Fig. 1(a), and (ii) pressure-driven displacement flow of one fluid by another one, shown in Fig. 1(b). Let us first discuss what happens in the single-component (SC) systems, i.e when the viscosity stratification is achieved by varying one species. In the first configuration, it is well known that the laminar flow becomes unstable if the highly viscous fluid occupies the near wall/annular region, whereas a huge stabilization occurs if the highly viscous fluid occupies the core region of the channel or pipe (Govindarajan, 2004; Joseph *et al*., 1997; Malik and Hooper, 2005; Sahu *et al*., 2009a, 2007; Selvam *et al*., 2007, 2009). In the second configuration, it is well established (Chouke *et al*., 1959; Saffman and Taylor, 1958; Sahu and Matar, 2010; Tan and Homsy, 1986) that if the displacing fluid is less viscous than the displaced one the interface separating them becomes unstable and fingering pattern (Saffman-Taylor instability (Saffman and Taylor, 1958)) develops at the interface. However, the situation when a highly viscous fluid displaces a less viscous fluid is generally stable. In this context, the review of instabilities observed in porous media and Hele-Shaw cells was conducted by Homsy (1987).

In the sections to come, we will discuss the effects of double-diffusive phenomena on these systems when we expect the flow to be stable in the context of single component systems. The equations governing the flow studied in this review are discussed in the next section. The results are discussed in section 3. Some concluding remarks are presented in section 4.

Formulation

The schematics of the flow configurations considered are shown in Fig. 1(a) and (b). In the core-annular/ three-layer flow (shown in Fig. 1(a)) it can be seen that the fluids '1' and '2' occupy the core and annular regions of the channel, respectively, and a mixed region of thickness, q, separates the fluids, where the concentration of the species and viscosity of the fluid varies gradually. In Fig. 1(b), the initial configuration of the pressure-driven displacement is shown. Here fluid '2' is occupying the entire channel initially, which is being displaced by another fluid (fluid '1') injected at the inlet of the channel. These fluids contain two differently diffusing species, say S and F, in different proportions, wherein S and F represent the slower and faster diffusing species. The diffusivity ratio $\delta \equiv \mathcal{D}_f/\mathcal{D}_s$ where $\mathcal{D}_s$ and $\mathcal{D}_f$ are the diffusion coefficients of the slower and faster diffusing species, thus $\delta \geq 1$. The concentrations of S and F in fluids '1' and '2' are S_1, F_1, and S_2, F_2, respectively, such that the net viscosity of fluids '1' and '2' are μ_1 and μ_2, respectively. The viscosity ratio, m is defined as μ_2/μ_1. We use the Cartesian coordinate system (x, y) where x and y denote the horizontal and vertical coordinates, respectively. The channel walls shown in Fig. 1(a) and (b) are assumed to be rigid and impermeable.

We assume an exponential dependence of the viscosity, μ on the concentration of the species:

$$\mu = \mu_1 \exp\left[R_s \left(\frac{S - S_1}{S_2 - S_1} \right) + R_f \left(\frac{F - F_1}{F_2 - F_1} \right) \right], \quad (1)$$

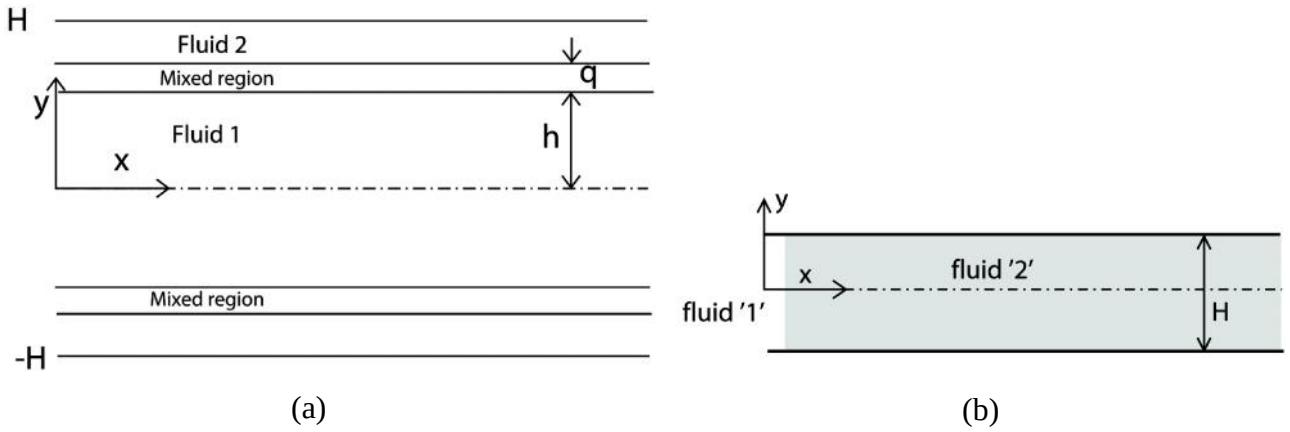

Fig. 1: Schematic of the three-layer configuration with the fluids '1' and '2' occupying the core and annular regions, respectively. The two fluids are separated by a mixed layer of uniform thickness *q*, with fluid '1' located in the region $-h \le y \le h$. (b) Schematic diagram showing the initial flow configuration of the displacement flow: initially fluid '2' occupies the entire channel, which is being displaced by fluid '1' (injected at the inlet of the channel)

where R_s ($\equiv (S_2 - S_1)\, d(\ln \mu)/dS$) and R_f ($\equiv (F_2 - F_1)\, d(\ln \mu)/dF$) are the log-mobility ratios of the scalars S and F, respectively. Thus, $R_s + R_f < 0$ represents situation when the annular fluid is less viscous than the core fluid in the core-annular flow (shown in figure 1(a)). In displacement flow (shown in Fig. 1(b)) it represents situation where the viscosity decreases as we move in the positive x direction in the mixed layer. The following scaling is used in order to non-dimensionize the governing equations:

$$
\begin{aligned}
&(x, y) = H(\tilde{x}, \tilde{y}), (q, h) = H(q, \tilde{h}), t = \frac{H^2}{Q}\tilde{t}, \\
&(u, v) = \frac{Q}{H}(\tilde{u}, \tilde{v}),\ p = \frac{\rho Q^2}{H^2}\, p,\ \mu = \tilde{\mu}\mu_1 \\
&\tilde{s} = \frac{S - S_1}{S_2 - S_1},\ \tilde{f}\,\frac{F - F_1}{F_2 - F_1},
\end{aligned}
\tag{2}
$$

where Q denotes the total volume flow rate per unit distance in the spanwise direction, $\mathbf{u} \equiv (u, v)$ is the velocity vector, u and v being its components in the x and y directions, respectively, ρ is the constant density, t is time and p denotes pressure. The tildes here designate dimensionless quantities, but are dropped for convenience in the dimensionless governing equations, given by

$$\nabla \cdot \mathbf{u} = 0, \tag{3}$$

$$\left[\frac{\partial \mathbf{u}}{\partial t} + \mathbf{u} \cdot \nabla \mathbf{u}\right] = -\nabla p + \frac{1}{\mathrm{Re}} \nabla \cdot [\mu(\nabla \mathbf{u} + \nabla \mathbf{u}^T)], \tag{4}$$

$$\left[\frac{\partial s}{\partial t} + \mathbf{u} \cdot \nabla s\right] = \frac{1}{\mathrm{Pe}} \nabla^2 s, \tag{5}$$

$$\left[\frac{\partial f}{\partial t} + \mathbf{u} \cdot \nabla f\right] = \frac{\delta}{\mathrm{Pe}} \nabla^2 f, \tag{6}$$

where $Re \equiv \rho Q/\mu_1$, $Pe \equiv Q/\mathcal{D}_s$ and $Sc \equiv Pe/Re$ are the Reynolds number, the Péclet number and Schmidt number, respectively.

Linear Stability Analysis of Core-Annular Flow

In order to conduct a linear stability analysis in core-annular flow (shown in Fig. 1(a)) one would assume an equilibrium basic state for the flow, which may correspond to a steady, parallel, fully-developed flow, such that $V = 0$, U is a function of y alone and P is linear in x. The flow is also considered to be symmetrical about the channel centerline. Thus, only top half of the channel is considered as a computational domain. Here the basic state quantities are designated by upper-case letters. The basic state concentration of the species s_0 and f_0 are chosen to be fifth order polynomials in the mixed layer, such that the concentrations are continuous up to the

second derivative at $y = h$ and $y = h + q$.

$$\begin{aligned} s_0 &= f_0 = 0, \quad 0 \le y \le h, \\ s_0 &= f_0 = \sum_{i=1}^{6} a_i y^{i-1}, \ h \le y \le h+q, \\ s_0 &= f_0 = 1, \quad h+q \le y \le 1, \end{aligned} \tag{7}$$

where a_i (i = 1, 6) are given by

$$a_1 = \frac{-h^3}{q^5}(6h^2 + 15hq + 10q^2),\ a_2 = \frac{30h^2}{q^5}(h+q^2),$$

$$a_3 = -\frac{30h}{q^5}(h+q)(2h+q),$$

$$a_4 = -\frac{10}{q^5}(6h^2 + 6hq + q^2),$$

$$a_5 = -\frac{15}{q^5}(2h+q) \text{ and } a_6 = \frac{6}{q^5}. \tag{8}$$

Knowing the basic concentration profile of the species (given in Eq. (7))) and the viscosity variation with s_0 and f_0 as $\mu_0 = e^{(R_s s_0 + R_f f_0)}$, one could solve the steady, fully-developed version of Eq. (4), i.e.,

$$\mathrm{Re}\left(\frac{dP}{dx}\right) = \frac{d}{dy}\left(\mu_0 \frac{dU}{dy}\right). \tag{9}$$

This is subject to no-slip and no-flux conditions at the wall and the centerline of the channel, respectively, one could obtain the basic state velocity profile, $U(y)$. The nondimensional pressure gradient dP/dx is fixed by using constant volumetric flow rate condition given by $\int_0^1 U dy = 1$.

The linear stability equations are derived using the standard approach (see e.g. Schmid and Henningson, 2001), by using a normal modes analysis and splitting the flow variables into basic state quantities and two-dimensional perturbations, designated by a hat:

$$\begin{aligned} (u, v, p, s, f)(x, y, t) = (U(y), 0, P, s_0(y), \\ f_0(y)) + (\hat{u}, \hat{v}, \hat{p}, \hat{s}, \hat{f})(y) e^{1(\alpha x - \omega t)}. \end{aligned} \tag{10}$$

Here $1 \equiv \sqrt{-1}$, α and $\omega (\equiv \alpha c)$ are the wavenumber and frequency of the disturbance, respectively, wherein c is the phase speed of the disturbance. In case of temporal stability analysis, α and ω are assumed to be real and complex, respectively, whereas in case of spatio-temporal stability analysis both the quantities are treated as complex. It is to be noted that a given mode is unstable if $\omega_i > 0$, stable if $\omega_i < 0$ and neutrally stable if $\omega_i = 0$. In Eq. (10), the perturbation viscosity is given by: $\hat{\mu} = \frac{\partial \mu_0}{\partial s_0}\hat{s} + \frac{\partial \mu_0}{\partial f_0}\hat{f}$. The amplitude of the velocity disturbances are then re-expressed in terms of a streamfunction $((\hat{u}, \hat{v}) = (\psi', -1\alpha\psi))$; the prime denotes differentiation with respect to y. Substitution of Eq. (10) into Eqs. (3)-(6), subtraction of the basic state equations, subsequent linearization and elimination of the pressure perturbation yields the following linear stability equations (Sahu and Govindarajan, 2011,2012), where the hat notation is suppressed:

$$\begin{aligned} &1\alpha\,\mathrm{Re}\left[(\psi'' - \alpha^2\psi)(U-c) - U''\psi\right] \\ &= \mu_0(\psi^{iv} - 2\alpha^2\psi'' + \alpha^4\psi) + 2\mu_0'(\psi''' - \alpha^2\psi') \\ &+ \mu_0''(\psi'' + \alpha^2\psi) + U'(\mu'' + \alpha^2\mu) + 2U''\mu' + U'''\mu, \end{aligned} \tag{11}$$

$$1\alpha\, Pe[(U-c)s - \psi s_0'] = (s'' - \alpha^2 s), \tag{12}$$

$$1\alpha\, Pe[(U-c)f - \psi f_0'] = \delta(f'' - \alpha^2 f). \tag{13}$$

Solutions of these equations are obtained subject to the boundary conditions

$$\psi = \psi' = s = f = 0 \quad \text{at } y = 1, \text{ and} \tag{14}$$

$$\psi' = \psi''' = s' = f' = 0 \quad \text{at } y = 0. \tag{15}$$

Eqs. (11)-(15) constitute an eigenvalue problem, which is solved using a Chebyshev spectral

collocation method (Canuto *et al.*, 1987) on a stretched grid (Govindarajan, 2004). In order to understand the convective and absolute instabilities, a spatio-temporal stability analysis (Briggs, 1964; Sahu *et al.*, 2009a; Sahu and Matar, 2011) is conducted. The procedure is briefly outlined below.

The linearised differential operator represents a dispersion relation in complex (ω, α) space. The response of the linearised system to an impulse perturbation is given by the corresponding Green's function, $G(x, y, t)$. For a particular mode, the long-time behaviour of G along different 'rays' for which x/t is constant, is then analyzed. In order to determine whether the flow is convectively or absolutely unstable, one first determines the so-called "absolute frequency," $\omega_0 = \omega(\alpha_0)$, where α_0 is the "absolute wavenumber," may be complex and satisfies

$$\frac{\partial \omega}{\partial \alpha}(\alpha_0) = 0. \tag{16}$$

This corresponds to the ray $x/t = 0$ or zero group velocity. The "absolute growth rate" (imaginary part of absolute frequency, $\omega_{0,i}$) measures disturbance growth or decay along the $x/t = 0$ ray, i.e., in a stationary reference frame. The flow is then said to (i) convectively unstable if $\omega_{0,i} < 0$, and (ii) absolutely unstable if $\omega_{0,i} > 0$.

Direct Numerical Simulation of Displacement Flow

In case of displacement flows (shown in Fig. 1(b)), Eqs. (3)-(6) are solved directly via an in-house finite-volume approach in a staggered grid using the no-slip and no-penetration conditions at the walls; the Neumann boundary condition is applied at the outlet. The velocity profile at the inlet of the channel is assumed to be fully-developed.

Numerical Approach

A staggered grid finite-volume approach is used in order to solve the system of Eqs. (3)-(6), in which the scalar variables (the pressure and concentrations of the species) are defined at the center of each cell and the velocity components are defined at the cell faces. The discretized governing equations are given by:

$$\frac{\mathbf{u}^* - \mathbf{u}^n}{\Delta t} = \frac{1}{p^{n+1/2}}\left\{-\left[\frac{3}{2}\mathcal{H}(\mathbf{u}^n) - \frac{1}{2}\mathcal{H}(\mathbf{u}^{n-1})\right]\right\}$$

$$+\frac{1}{2\,\mathrm{Re}}\left\{\left[\mathcal{L}(\mathbf{u}^*, \mu^{n+1}) + \mathcal{L}(\mathbf{u}^n, \mu^n)\right]\right\}, \tag{17}$$

where $\mathbf{u}^*$ is the intermediate velocity, and $\mathcal{H}$ and $\mathcal{L}$ denote the discrete convection and diffusion operators, respectively. $\Delta t = t^{n+1} - t^n$ and the superscript n signifies the discretized nth step.

The intermediate velocity $\mathbf{u}^*$ is then corrected to $(n + 1)$th time level.

$$\frac{\mathbf{u}^{n+1} - \mathbf{u}^*}{\Delta t} = \nabla p^{n+1/2}. \tag{18}$$

Here, in order to achieve second-order accuracy in the temporal discretization, the Adams-Bashforth and the Crank-Nicolson methods are used for the advective and second-order dissipation terms in Eq. (4), respectively.

The pressure distribution is obtained from the continuity equation at time step $n + 1$ using

$$\nabla \cdot (\nabla p^{n+1/2}) = \frac{\nabla \cdot \mathbf{u}^*}{\Delta t}. \tag{19}$$

The discretized diffusion equations of the slower and faster diffusing species are

$$\frac{\frac{3}{2}s^{n+1} - 2s^n + \frac{1}{2}s^{n-1}}{\Delta t} = \frac{1}{\mathrm{Re\,Sc}}\nabla^2 s^{n+1}$$
$$-2\nabla \cdot (\mathbf{u}^n s^n) + \nabla \cdot (\mathbf{u}^{n-1} s^{n-1}), \tag{20}$$

$$\frac{\frac{3}{2}f^{n+1} - 2f^n + \frac{1}{2}f^{n-1}}{\Delta t} = \frac{\delta}{\mathrm{Re\,Sc}}\nabla^2 f^{n+1}$$
$$-2\nabla \cdot (\mathbf{u}^n f^n) + \nabla \cdot (\mathbf{u}^{n-1} f^{n-1}), \tag{21}$$

respectively. In Eqs. (20) and (21), the weighted essentially non-oscillatory (WENO) and the central

difference schemes are used to discretize the advective terms and the diffusive terms of Eqs. (5)-(6).

The readers are also refereed to our previous papers (Mishra *et al*., 2012; Sahu and Govindarajan, 2011, 2012) for details of the numerical approach used and the validation of the present solver.

Results and Discussion

Core-Annular/Three-Layer Flow

1. Single-Component System

For unstratified flow in channel, it is well known that the critical Reynolds number, Re_{cr} (*Re* at which the flow becomes linearly unstable) is 3848.13, which is defined based on the average velocity profile and half-width of the channel (Drazin and Reid, 1985). The most unstable mode in this case is known as Tollmein-Schlichting (TS) instability wave.

Before discussing the DD effect on viscosity stratified systems, let us first discuss the linear instability characteristics of single-component (SC) flows (i.e. when the viscosity stratification is achieved only due to one species) in a channel. Govindarajan *et al*. (2001), and Ranganathan and Govindarajan (2001) were the first to study the linear instability of viscosity-stratified three-layer SC channel flow. A representative result from the study of Govindarajan (2004) is shown in Fig. 2(a), where the critical Reynolds number, Re_{cr} is plotted versus the Schmidt number *Sc* for different values of viscosity ratio. Here $m > 1$ ($m < 1$) represents a situation where the viscosity of the fluid decreases (increases) in the mixed region as we move away from the wall. It can be seen in Fig. 2(a) that for all values of *m* less than 1 the critical Reynolds number is higher than 3848.13 (shown by red dotted line in Fig. 2(a)), which means that the flow stabilizes when the annular fluid is less viscous than the core fluid. The opposite happens for all values of *m* greater than 1 confirming that if the annular fluid is more viscous then the core one, the flow destabilizes. This is due to the fact that for $m > 1$ the basic state velocity profile has tendency to become inflectional (i.e. after some positive value of *m*, *U*'' undergoes a sign change at some *y* location) and by Rayleigh theorem of inviscid instability criterion (Rayleigh, 1880) the flow becomes inviscidly unstable. On the other hand, the basic state velocity profile becomes 'fuller' (moves away from inflectional) for $m < 1$ and the flow becomes progressively more stable with decreasing viscosity ratio.

In Fig. 2(b) the regions of convective and absolute instabilities in a three-layer channel flow are shown for two values of *Sc* in viscosity ratio and

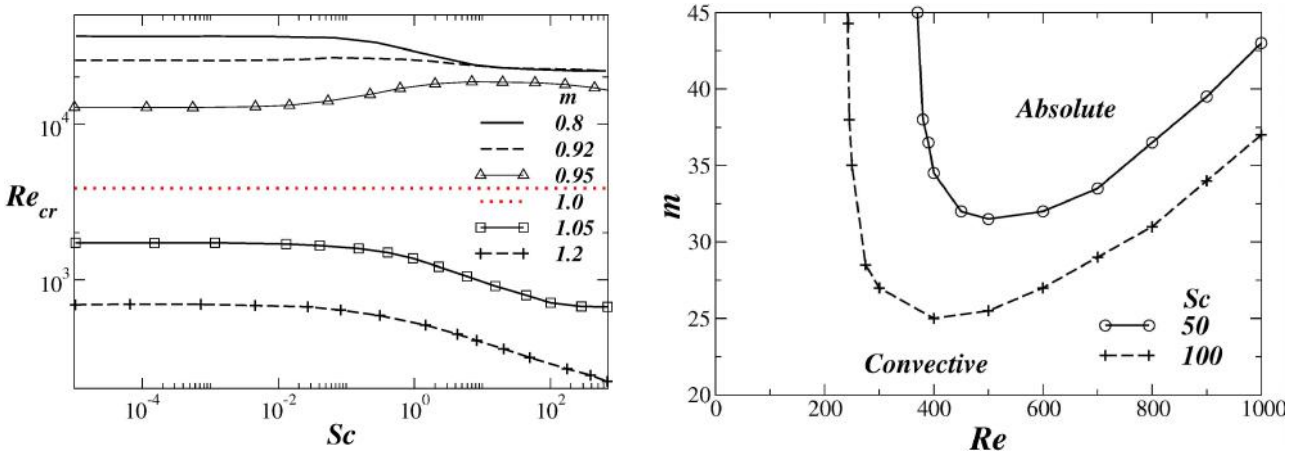

Fig. 2: Re_{cr} **versus** *Sc* **(reproduced with permission from Govindarajan, 2004). (b) Stability diagram showing the regions of convective and absolute instability in** *m*-*Re* **space for** $h = 0.3$ **and** $q = 0.05$ **(reproduced with permission from Sahu** ***et al*****., 2009a). The red dotted line (for** $m = 1$**) in panel (a) represents** $Re_{cr} = 3848.11$**.**

Reynolds number space. In a convectively unstable flow, the disturbance grows as it advect in the downstream direction of the flow. In contrast, when the flow is absolutely unstable the disturbance grows locally and spreads in both the upstream and downstream of the flow, which makes the entire regime unstable eventually. Sahu *et al*. (2009a) found that the flow becomes absolutely unstable when the annular fluid has a much higher viscosity as compared to that of the core fluid. A similar analysis was also conducted by Selvam *et al*. (2009) for a core-annular pipe flow. The demonstration to identify the nature of instability is provided in the next section.

Thus in summary, the dogmata in three-layer flows are:

- If $u_2 > u_1$, i.e., $m > 1$ the flow is more unstable than the corresponding unstratified case.
- On the other hand, if $u_2 < u_1$, i.e $m < 1$ the flow is more stable than the corresponding unstratified case.

2. Double-Diffusive Effect

Now let us consider a system, where the annular fluid is less viscous than that of the core fluid ($u_2 < u_1$) in the presence of double-diffusive effect (when both the slower and faster diffusing species contribute to the viscosity stratification). As discussed above, in the context of single component flow this configuration is more stable than the unstratified channel flow.

In Fig. 3(a), the neutral stability boundaries (α versus *Re*) for different values of δ (which represents the diffusivity ratio of the species) are plotted. These curves provide the minimum values of the Reynolds number for which the flow is linearly unstable, Re_{cr} for different values of δ. The boundaries on the right hand side of Fig. 3(a) corresponds to the Tollmien-Schlichting (TS) mode, whereas the 'egg-shaped' boundaries on the left hand side correspond to the double-diffuse (DD) mode. As expected, it can be seen that for $\delta = 1$, the flow is dominated by the TS mode only. For $\delta > 1$ a new ('egg-shaped') mode of instability due to the double-diffusive effect appears at lower Reynolds numbers. It can also be observed that increasing δ increases this region of instability due to DD effect and Re_{cr} decreases with increasing the value of δ.

In Fig. 3(a), the mechanism of the instability is broadly analogous to the fingering instability of gravity-driven convection. In this case the net stratification is stabilising ($R_s + R_f < 0$) according to our intuition, with slower-diffusing species (*S*) destabilizing ($R_s > 0$) and faster-diffusing species (*F*) stabilizing ($R_f < 0$). Consider a small parcel of fluid from the annular region displaced vertically in to the region of core fluid. The resulting perturbation in *F*

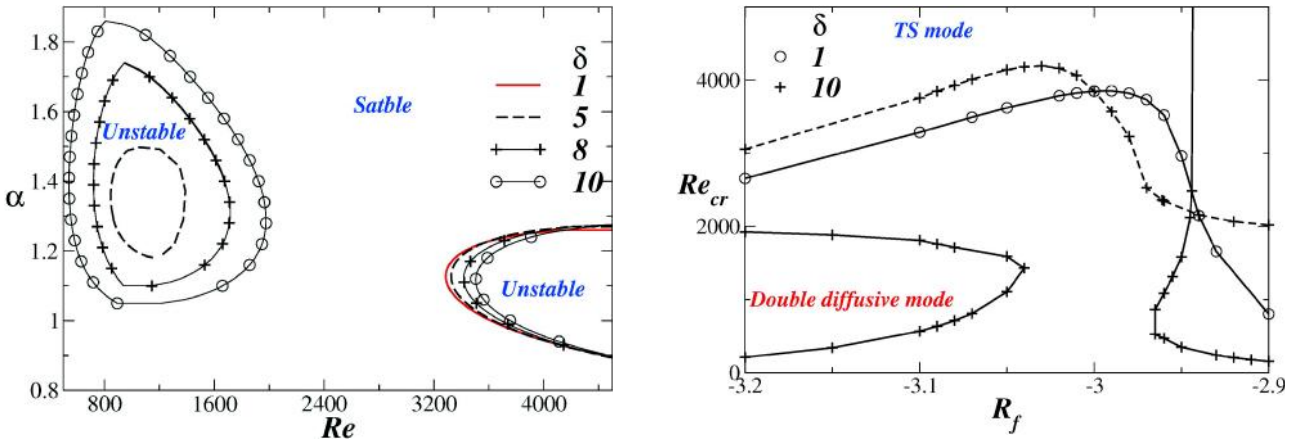

Fig. 3: (a) Effect of δ on the neutral stability curves. The parameter values are *Sc* = 30, *h* = 0.7, *q* = 0.1, R_s = 3 and R_f = –3.1. Note that the DD mode is not present for δ = 1 (shown by red line). (b) The stability diagram showing the effect of R_f on the critical Reynolds number, Re_{cr} for R_s = 1, *h* =0.7, *q* = 0.1 and *Sc* = 50. This figure is reproduced with permission from Sahu and Govindarajan (2011)

will diffuse away faster, leaving the destabilizing effect of *S*, which causes the DD mode.

Now intuitively less obvious is the existence of DD instability, where *F* is destabilizing ($R_f > 0$) and *S* stabilizing ($R_s < 0$). A similar 'egg-shaped' unstable mode (not shown) is also observed when $R_f > 0$ and $R_s < 0$ for $\delta > 1$. This case is in broad analogy with the diffusive regime in DD convection. A displaced parcel would now tend to return to its old position but, due to the diffusing away meanwhile of the *F* perturbation and the corresponding decrease in viscosity, would tend to overshoot its original location resulting in an oscillatory instability. Sahu and Govindarajan (2011) also demonstrates that an overlap of the critical layer, y_c (where the value of *U* equals to the phase speed (ω/α) of the most unstable disturbance with the stratified layer is necessary for the DD mode to be destabilized effectively. In most of the cases considered here $y_c \sim 0.7$. The region of the TS and DD modes are presented in Fig. 3(b) for different values of the log-mobility ratio of the faster-diffusing species, R_f.

It is also noted here that the thickness of stratification region, *q* plays a significant role in the stability behaviour. When $q = 0$, i.e., in the presence of sharp interface (for $Sc \to \infty$), another mode, commonly known as Yih mode, appears in viscosity stratified flows, which is unstable at any Reynolds number (Yih, 1967). For miscible flows (with finite Schmidt number) increasing the thickness of stratification region has a stabilizing influence (Ern *et al*., 2003).

However, the stability characteristics of the TS and DD modes in the single-component and double-diffusive cases qualitatively remain unchanged for $0.05 \le q \le 0.2$ (Govindarajan, 2004; Sahu and Govindarajan, 2011).

Sahu and Govindarajan (2012) also conducted the spatio-temporal stability analysis discussed in the previous section. In order to know whether the flow is convectively or absolutely unstable the isocontours of ω_i is plotted in complex α plane. The value of ω_i at the saddle point, $\omega_{0,i}$ decides the nature of these instabilities, as discussed in Section 2. In Fig. 4, we compare the isocontours of ω_i for a DD case and the equivalent SC system. The equivalent SC system has the same average diffusivity as the DD system. Thus $\mathcal{D}_{SC} = (\mathcal{D}_s + \mathcal{D}_f)/2$; so the equivalent Schmidt number

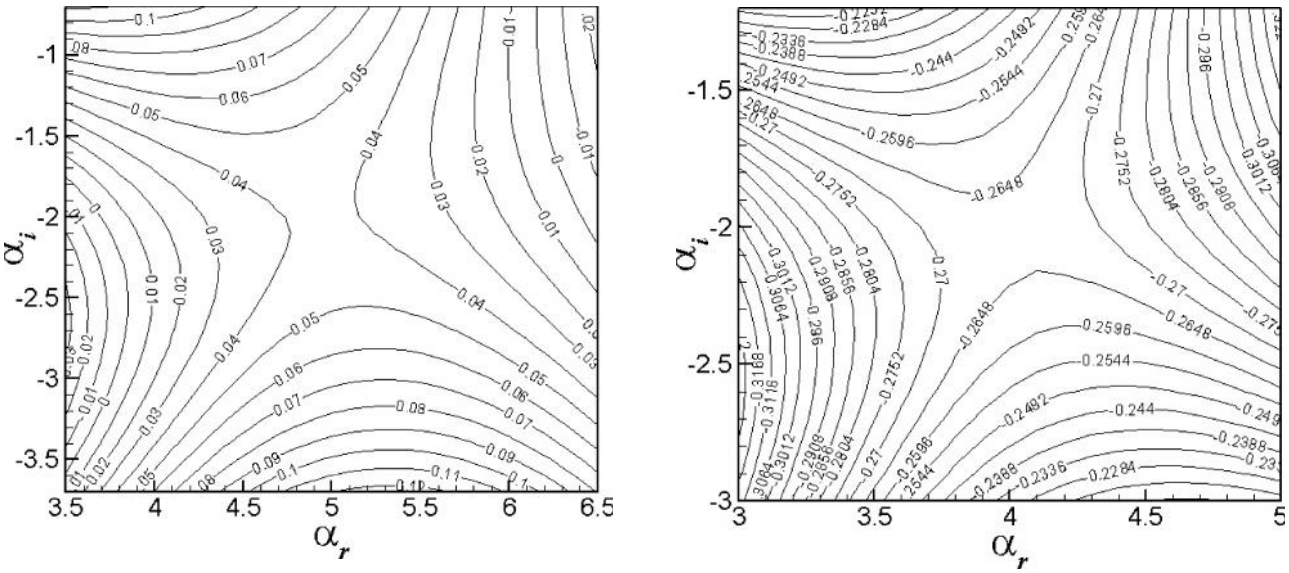

Fig. 4: Isocontours of ω_i in the complex wavenumber plane for (a) a DD system (Re = 200, Sc = 50, δ = 10, h = 0.6, q = 0.1, R_s = 4 and R_f = –0.5), (b) single component system equivalent to the double-diffusive system shown in panel (a) (Re = 200, Sc = 9.091, h = 0.6, q = 0.1, R_s = 3.5 and R_f = 0). The maximum temporal growths, ω_{max} in each case is positive. The frequency at the saddle point, ω_0 are 1.156 + 0.041i and 1.265 – 0.266i. This shows that flow is absolutely unstable in panel (a), but convectively unstable in panel (b). This figure is reproduced with permission from Sahu and Govindarajan (2012)

of the SC flow is given by $2Sc/(1 + \delta)$. It can be seen in Fig. 4 that the value of $\omega_{0,i}$ for the DD case is positive, on the other hand, for the equivalent SC case it is negative. This result confirms that DD effect makes the flow absolutely unstable for the parameter values considered in generating Fig. 4. Following this procedure, Sahu and Govindarajan (2012) also identify the convectively and absolutely unstable regimes in the presence of DD effect (shown in Fig. 5).

Displacement Flow

Now let us consider the second configuration (shown in Fig. 1(b)), wherein one fluid is displaced by another one. Several earlier studies (Chouke *et al*., 1959; Saffman and Taylor, 1958; Tan and Homy, 1986) have shown that if the displacing fluid is less viscous than the displaced fluid, the interface separating the fluids becomes unstable and finger like structures develop at the interface. Recently, this phenomenon has been numerically investigated by Sahu and co-workers (Redapangu *et al*., 2012, 2013; Sahu *et al*., 2009a,b) in pressure-driven displacement flow of one fluid by another in two and three-dimensional channels using finite-volume and lattice Boltzmann approaches. They also found that if the invading fluid is less viscous than the resident fluid, the flow becomes unstable and Kelvin-Helmholtz type instabilities appear at the interface separating the fluids. On the other hand, when a highly viscous fluid displaces a less viscous one, it was found to be stable.

Mishra *et al*. (2010) ware the first to conduct numerical simulation of displacement flow in porous media in the presence of two species diffusing at different rates. Solving the Darcy equation and the diffusion equations for both the species, they found that the fingering patterns appear in the mixed region even when a highly viscous fluid displaces a less viscous one (shown in Fig. 6). This is an interesting result. However, in porous media the inertia is neglected and the flow dynamics is controlled by diffusion only.

Thus we ask a question: whether a similar type of instability due to the double-diffusive effect are present in systems where inertia also plays an equally important role as that of diffusion.

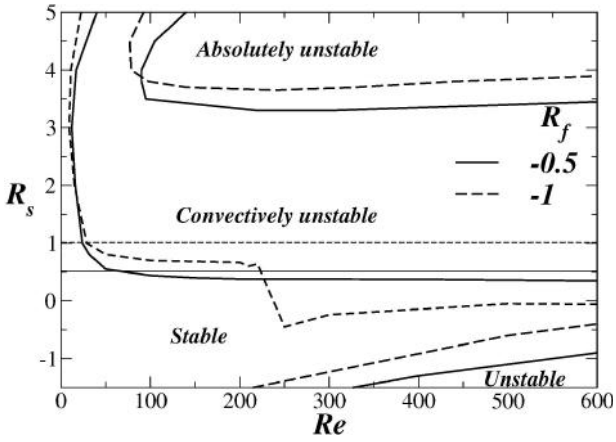

Fig. 5: Stability diagrams showing the regions of convective and absolute instabilities in R_s-Re space for Sc = 50, δ =10, h = 0.6 and q = 0.1. The horizontal line show the location where $R_s + R_f = 0$. Above this line, the average viscosity increases as we move from the centerline of the channel towards the wall. This figure is reproduced with permission from Sahu and Govindarajan (2012)

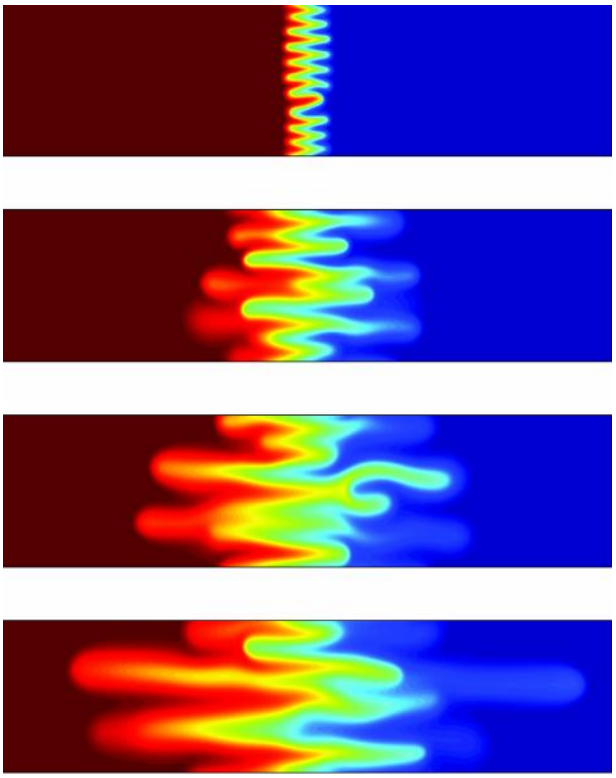

Fig. 6: Displacement flow of a less viscous fluid (shown by blue) by a highly viscous fluid (shown by red) in porous media at different time (time increases as we go down). This figure is reproduced with permission from Mishra *et al.* (2010).

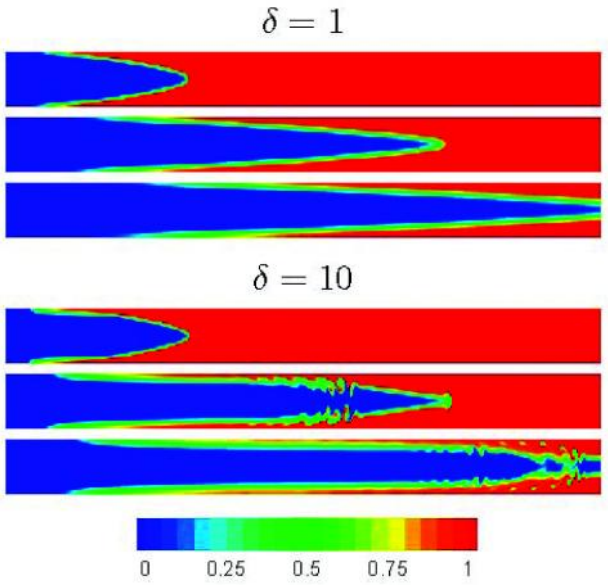

Fig. 7: Spatio-temporal evolutions of the concentration field of the scalar *s* at successive times (from top to bottom in each panel: *t* = 20, 50 and 75). The color-map is shown at the bottom. The rest of the parameter values are Re = 100, Sc_s = 100, R_s = 3 and R_f = –3.6. This figure is reproduced with permission from Mishra *et al*. (2012)

The direct numerical simulation of Eqs. (3)-(6) was conducted for pressure-driven channel flow of a less viscous fluid by a highly viscous one, injected at the inlet of the channel, shown in Fig. 1(b). One of the main result of Mishra *et al*. (2012) showing the spatio-temporal evaluation of the concentration field of the slower diffusing species is presented in Fig. 7. In this configuration at t = 0 the log-mobility ratios are specified such that the viscosity decreases monotonically as we move in the downstream direction. As discussed above this is a classically stable configuration in the context of single component flows. As expected, it can be seen that for δ = 1 (SC flow) a finger of a highly viscous fluid penetrates inside the channel, which forms a 'pure-Poiseuille-diffusive' structure. However, for δ = 10 it can be observed that the finger of the highly viscous fluid becomes unstable forming a 'cap-like' structure at the tip of the finger, which grows with time, and also at later times the Kelvin-Helmholtz type instabilities at the interface separating the fluids are also apparent at the top and bottom part of the finger. In this study, the diffusion coefficients of the species are considered to be constant, although diffusivity is a function of viscosity when viscosity ratio is high. Recently Sahu (2013) studied the influence of variable diffusivity (Stokes-Einstein relationship, $\mathcal{D} = C/\mu$ on the flow dynamics and found that bigger 'cap-like' instability appears in the variable-diffusivity case.

In order to understand the mechanism, they also plotted the axial variation of the transverse averaged viscosity, $\bar{\mu} \equiv \int_0^1 \mu dy$ for different times (shown in Fig. 8(a) and (b)) for δ = 1 and 10. It can be observed

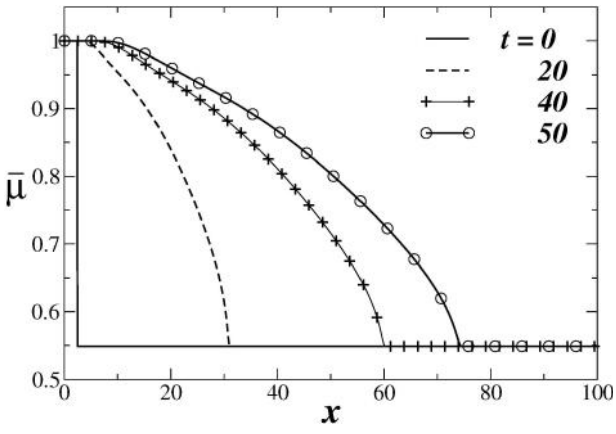

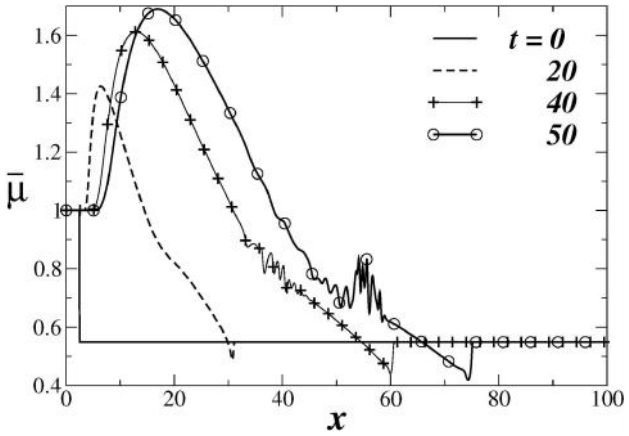

Fig. 8: Axial variation of transverse averaged viscosity $\bar{\mu} = \int_0^1 \mu dy$. The panels (a), and (b) represent the results for δ = 1 and δ = 10, respectively. The rest of the parameter values are the same as those used to generate Fig. 7. This figure is reproduced with permission from Mishra *et al*. (2012)

in Fig. 8(a) that for $\delta = 1$, $\bar{\mu}$ decreases monotonically for all the times. This shows that at any time in the flow we have highly viscous fluid displacing a less viscous one. For $\delta = 10$ it can be seen that $\bar{\mu}$ varies non-monotonically in the axial direction at the later times. This creates local maxima in the flow domain. Thus although in the initial configuration we have a highly viscous fluid displacing the less viscous fluid, one could locally have an opposite situation (less viscous fluid displacing the highly viscous one). This resultant flow is an unstable configuration, which has been discussed above. This is the main reason why due to the DD effect we get instability in a classically stable configuration in the context of single component flows.

Concluding Remarks

In this paper, the previous work on the instability due to double-diffusive effect is reviewed. Two configurations, namely core-annular flow with the less viscous fluid occupying the annular region, and pressure-driven flow of a less viscous fluid by a highly viscous fluid in a channel are investigated. These flow configurations are known to be stable in the context of single-component flows, but becomes unstable in the presence of double-diffusive effects. Since these DD instabilities take the form of Saffman-Taylor instabilities as suggested in Fig. 8(b), the dogma in single-component flows are not fundamentally relevant in this case.

Acknowledgments

The author thanks the support from Department of Science and Technology, India for their financial support (Grant No: SR/FTP/ETA-85/2010). Profs. Rama Govindarajan, Omar K. Matar, Manoranjan Mishra and Anne De Wit are gratefully acknowledged for the collaboration in conducting some of the studies presented in this review. I also thank Profs. Sumohana Channappayya and Harish Dixit of IIT Hyderabad for giving valuable suggestions.

References

Briggs R J (1964) Research monograph no. 29 MIT Press, Cambridge

Canuto C, Hussaini M Y, Quarteroni A and Zang T (1987) Spectral Methods in Fluid Dynamics, 1st Edition. Springer-Verlag, Amsterdam

Chouke R, Van Meurs P and Van Der Pol C (1959) The instability of slow, immiscible, viscous liquid-liquid displacements in permeable media *Trans AIME* **216** 188-194

Drazin P G and Reid W H (1985) Hydrodynamic stability. Cambridge University Press, Cambridge

Ern P, Charru F and Luchini P (2003) Stability analysis of a shear flow with strongly stratified viscosity *J Fluid Mech* **496** 295-312

Govindarajan R (2004) Effect of miscibility on the linear instability of two-fluid channel flow *Int J Multiphase Flow* **30** 1177-1192

Govindarajan R, L'vov S V and Procaccia I (2001) Retardation of the onset of turbulence by minor viscosity contrasts *Phys Rev Lett* **87** 174501

Govindarajan R and Sahu K C (2014) Instabilities in viscosity-stratified flows *Ann Rev Fluid Mech* **46** 331-353

Homsy G M (1987) Viscous fingering in porous media *Ann Rev Fluid Mech* **19** 271-311

Joseph D D, Bai R, Chen K P and Renardy Y Y (1997) Core-annular flows *Ann Rev Fluid Mech* **29** 65-90

Malik S V and Hooper A P (2005) Linear stability and energy growth of viscosity stratified flows *Phys Fluids* **17** 024101

Mishra M, De Wit A and Sahu K C (2012) Double diffusive effects on pressure-driven miscible displacement flows in a channel *J Fluid Mech* **712** 579-597

Mishra M, Trevelyan P M J, Almarcha C and De Wit A (2010) Influence of double diffusive effects and miscible viscous fingering *Physical review letters* **105** 204501

Ranganathan B T and Govindarajan R (2001) Stabilisation and destabilization of channel flow by location of viscosity-stratified fluid layer *Phys Fluids* **13**(1) 1-3

Rayleigh L (1880) On the stability of certain fluid motions *Proc Lond Maths Soc* **11** 57-70

Redapangu P R, Sahu K C and Vanka S P (2012) Study of pressure-driven displacement flow of two immiscible liquids using a multiphase lattice Boltzmann approach *Phys Fluids* **24** 102110

Redapangu P R, Sahu K C and Vanka S P (2013) A lattice Boltzmann simulation of three-dimensional displacement

flow of two immiscible liquids in a square duct *J Fluids Eng* **135** 121202

Saffman P and Taylor G (1958) The penetration of a finger into a porous medium in a Hele-Shaw cell containing a more viscous liquid *Proc Roy Soc Lond A* **245** 312-329

Sahu K C (2013) Double diffusive effects on pressure-driven miscible channel flow: Influence of variable diffusivity *Int J Multiphase Flow* **55** 24-31

Sahu K C, Ding H, Valluri P and Matar O K (2009a) Linear stability analysis and numerical simulation of miscible channel flows *Phys Fluids* **21** 042104

Sahu K C, Ding H, Valluri P and Matar O K (2009b) Pressure-driven miscible two-fluid channel flow with density gradients *Phys Fluids* **21** 043603

Sahu K C and Govindarajan R (2011) Linear stability of double-diffusive two-fluid channel flow *J Fluid Mech* **687** 529-539

Sahu K C and Govindarajan R (2012) Spatio-temporal linear stability of double-diffusive two-fluid channel flow *Phys Fluids* **24** 054103

Sahu K C and Matar O K (2010) Stability of plane channel flow with viscous heating *J Fluids Eng* **132** 011202

Sahu K C and Matar O K (2011) Three-dimensional convective and absolute instabilities in pressure-driven two-layer channel flow *Int J Numer Meth Fluids* **37** 987-993

Sahu K C, Valluri P, Spelt P D M and Matar O K (2007) Linear instability of pressure-driven channel flow of a Newtonian and Herschel-Bulkley fluid *Phys Fluids* **19** 122101

Schmid P J and Henningson D S (2001) Stability and Transition in Shear Flows. Springer, New York.

Selvam B, Merk S, Govindarajan R and Meiburg E (2007) Stability of miscible core-annular flows with viscosity stratification *J Fluid Mech* **592** 23-49

Selvam B, Talon T, Lesshafft L and Meiburg E (2009) Convective/absolute instability in miscible core-annular flow. part 2. numerical simulations and nonlinear global modes *J Fluid Mech* **618** 323-348

Tan C T and Homsy G M (1986) Stability of miscible displacements: rectangular flow *Phys Fluid* **29** 3549-3556

Turner J S (1974) Double-diffusive phenomena *Annual Review of Fluid Mechanics* **6** 37-54

Yih C S (1967) Instability due to viscous stratification *J Fluid Mech* **27** 337-352.